

Manufacturing of AA7075 Aluminum Alloy Composites Reinforced by Nanosized Particles of SiC, TiN, and ZnO by High-Energy Ball Milling and Hot Extrusion

Heronilton Mendes de Lira^{a*} , Wésia Amanda de Oliveira Barbosa^a,

Euclides Apolinário Cabral de Pina^b, Alexandre Douglas Araújo de Moura^b, Pilar Rey Rodriguez^c,

Ivanilda Ramos de Melo^d , Oscar Olímpio de Araújo Filho^d

^aUniversidade Federal Rural de Pernambuco (UFRPE), Unidade Acadêmica de Belo Jardim (UABJ), Belo Jardim, PE, Brasil.

^bUniversidade Federal Rural de Pernambuco (UFRPE), Unidade Acadêmica de Cabo de Santo Agostinho (UACSA), Cabo de Santo Agostinho, PE, Brasil.

^cAIMEN Centro Tecnológico, Porriño-Pontevedra, Spain.

^dUniversidade Federal de Pernambuco (UFPE), Recife, PE, Brasil.

Received: February 28, 2023; Revised: June 09, 2023; Accepted: September 01, 2023

In this work, composite powders of aluminum alloy 7075 (AA7075) reinforced by 2 weight percent of nanosized particles of silicon carbide (SiC), titanium nitride (TiN), and zinc oxide (ZnO) were produced in a bath of isopropyl alcohol by high energy ball milling during 480 min at 25 °C, 900 rpm, and Balls-to-Powder Weight Ratio (BPR) of 20:1. The techniques of X-Ray Diffraction (XRD), Laser Diffraction Method (LDM), Scanning Electron Microscopy (SEM), and microanalysis of Energy Dispersive Spectroscopy (EDS) were used to characterize the powders as received and processed. Then, the composites were hot extruded and characterized by XRD, SEM, and microhardness Vickers (HV). The milling process reduces the crystallite and particle size to around 30 nm and 10 μm, respectively. After extrusion, a fine microstructure and good consolidation were found for all bars, except for AA7075 as received. The ranging microhardness values were from 97 HV to 121 HV.

Keywords: Nanostructured Composites, Powder Metallurgy, Hot Extrusion.

1. Introduction

A composite combines two or more different materials to obtain a new material with unique characteristics. The type, variation, and interaction of reinforcement in the matrix are vital in determining the final properties¹.

Nanostructured metallic matrix composites usually combine the ductility of the metal (matrix) with ceramic particles (reinforcements) to enhance the mechanical properties to values found in the material of responsibilities². For example, the aluminum alloy matrix can promote characteristic properties of high strength stiffness to weight ratio, good formability, corrosion resistance, and recycling potential, making it the ideal candidate to replace heavier materials like steel or copper in other applications. In this context, the aluminum alloy 7075 matrix can support high-stress structural due to the formation of MgZn₂ precipitates. At the same time, SiC particle reinforcements can promote a significant strength, TiN increases the self-life of material, and ZnO improves the substrate coating³⁻⁸.

The powder metallurgy route can manufacture nanostructured composites using High-Energy Ball Milling (HEBM) technique. The process has a significant advantage in grain and particle reinforcement because it utilizes high-frequency impacts causing severe plastic deformation, cold welding of the particles, and repeated fracturing⁹. HEBM introduces shear bands that contain

a high-density network of dislocations and other crystallite defects that reduces crystallite and particle size and promotes changes in morphology before reaching the equilibrium state¹⁰⁻¹³. Special attention is paid to studying the influence of the medium on the milling process when developing ball-milling methods. Composites milled in a liquid medium can present finer ground than achieve dry milling due to how the nanoparticles are dispersed in the matrix. Moreover, HEBM in a liquid media can increase the contamination of the process and decrease the surface energy of particles¹⁴⁻¹⁹.

The hot extrusion technique is suitable for consolidating powdered material and excluding the sintering step. Usually, it requires elevated pressures and temperatures to reach desired quality and microstructure. On the other hand, the parameters of extrusion, such as the force applied, the billet temperature, and the extrusion speed, are primary factors influencing the quality of the specimens²⁰. It is an efficient route to manufacture aluminum alloy composites reinforced with ceramic phases with good densification^{21,22}.

Therefore, this paper focuses on manufacturing AA7075 metal matrix composite reinforced with nanosized particles of SiC, TiN, or ZnO produced by high-energy ball milling and hot extrusion. The aim is to evaluate the effects of milling in a bath of isopropyl alcohol at room temperature and reinforcements on the microstructure before and after extrusion and the microhardness of the extruded bars.

*e-mail: heronilton.lira@ufrpe.br

The control of these parameters is fundamental to producing a nanostructured composite with better performance.

2. Experimental Procedure

2.1. Manufacturing and characterization of powders

AA7075 powders with 99.7 % purity, supplied by Aluminum Powder Corporate, have been used as matrices. The initial particle size obtained by LDM was 31.7 μm (D50), and the crystallite size measured by XRD was 49 nm. According to manufacturer, the chemical composition in weight percentual is in Table 1.

Three nanometric powders have been used as reinforcements. The nanoparticle sizes were informed by the manufacturers: SiC, with a D50 of 50 nm (supplied by Iolitec GMBH), TiN, with a D50 of 20 nm (supplied by Iolitec GMBH); and ZnO, with a D50 of 100 nm (supplied by Sigma – Aldrich Corporate).

For each batch, 50 g of nanocrystalline powders AA7075 alloy was put in stainless steel attritor mill developed by the UFPE, equipped with a K-type thermocouple and a temperature controller. In all cases, milling was carried out for 480 minutes at 900 rpm, with a 20:1 ball-to-powder weight ratio (BPR) using 6.4 mm stainless steel balls 100C6 (1 %C, 1.5 %Cr), 1 wt% of zinc stearate (C₃₆H₇₀O₄Zn) as process control agent (PCA), a bath of 100 ml isopropyl alcohol (C₃H₇OH – 99.82 %) as liquid media milling, and the process temperature (25 °C) maintained via a water refrigerated jacket, around the attritor mill²³.

The reinforcements have the same concentration of 2 wt% for comparative purposes. This final percentage follows a previous work developed using TiC demonstrating that crystallite size diminished as reinforcement concentration increased from 0.5 to 2 wt%²⁴.

After milling, all the samples were dried at 100 °C to evaporate the alcohol completely²⁵. Then, the crystallite size, particle size, and morphology were analyzed.

XRD (Shimadzu XRD - 7000) investigated the crystallite size in the 2-Theta range from 5° - 120° with a scan rate of 0.02 °/s at 40 kV and 30 mA. The linear regression of the Williamson – Hall plot equation^{26,27} (Equation 1) was used to calculate the crystallite size and the contribution of micro deformation to the Full Width at Half Maximum (FWHM) of the four principal peaks of aluminum for a confidence factor of more than 92 percent. The experiment did not consider the instrument's effect on crystallite size comparatively.

$$FWHM = k\lambda / L\cos\theta + 4\varepsilon \tan\theta \quad (1)$$

Where “FWHM” is the full width at half maximum in radians; “k” is a constant (0.94); “ λ ” is the wavelength of the x-rays (15.4nm); “L” is the average crystallite size; “ θ ” is the Bragg angle, and “ ε ” is the micro deformation measured.

Laser Diffraction Method, LDM (Malvern Mastersizer 2000) determined the particle size. The sample was suspended in alcohol or water and agitated by ultrasound^{28,29}.

SEM - Hitachi TM 3000 operating at 20 kV, equipped with an EDX probe, analyzed the morphology and composition of the particles.

2.2. Hot extrusion consolidation and extruded bars characterization

All the composite powders were cold compressed as billets at the force of 35 kN during 120 s and compression speed of 1 kN/s. The billets were placed in a mold equipped with resistors to 450 °C. The billets were extruded in a relation of 25:1 at a speed of 1 mm/s to obtain bars of 5 mm diameter³⁰⁻³³ (Figures 1-3). Furthermore, boron nitride (BN) was used as a solid lubricant due to its chemical inertness, high-temperature stability (1000 °C), good thermal conductivity, and electrical insulation to avoid sticking during extrusion³⁴.

XRD, SEM, and Vickers microhardness characterized the extruded bars. Shimadzu HMV-2 durometer (HV 0.05) performed the microhardness according to ASTM E-384³⁵. XDR and SEM equipment were the same as those used for powder characterization.

3. Results and Discussion

3.1. Characterization of AA 7075 non-reinforced and reinforced composite powders

All the results are presented to compare the AA7075 powders received, milled, and alloyed milled with the different types of nano-reinforcements (composite powders). Table 2 shows crystallite and particle sizes, Figure 4 shows the diffractograms, and Figure 5 presents the particle size distribution.

After gridding, the diffraction peaks became broader and minor. The crystallite size decreased from 49nm to around 30nm, even without any reinforcement, because of the cold-welding phenomenon and repeated fractures³⁶. Besides that, the medium particle size decreased from D50 of 31.7 μm to around 10 μm , and micro deformation increased from 0.02 percent to around 0.12 percent.



Figure 1. Cold compressed billet before extrusion.

Table 1. Values of chemical composition of AA7075 powders.

Material	Weight (%)								
	Si (max)	Fe (max)	Cu	Mn (max)	Mg	Cr	Zn	Ti (max)	Al
AA7075	0.4	0.5	1.2-2.0	0.3	2.1-2.9	0.18- 28	5.1-6.1	0.2	Balance

Table 2. Values of crystallite, micro deformation, and particle size AA7075 (25 °C, 480 min, 900 rpm, 20:1 BPR): As received, milled, reinforced with 2 wt% SiC, TiN, and ZnO (Composites).

Samples	Crystallite Size [nm]	Micro Deformation [%]	Particle Size [μm]	Reinforce
AA7075 As received	49	0.02	31.71	No
AA7075 Milled	29	0.12	10.64	No
AA7075 Milled	32	0.10	13.66	2 % SiC
AA7075 Milled	29	0.12	9.25	2 % TiN
AA7075 Milled	30	0.12	10.40	2 % ZnO



a)



b)

Figure 2. a) Extrusion mold equipped with resistors; b) Mold placed in a compression machine.



Figure 3. Example of the bar extruded.

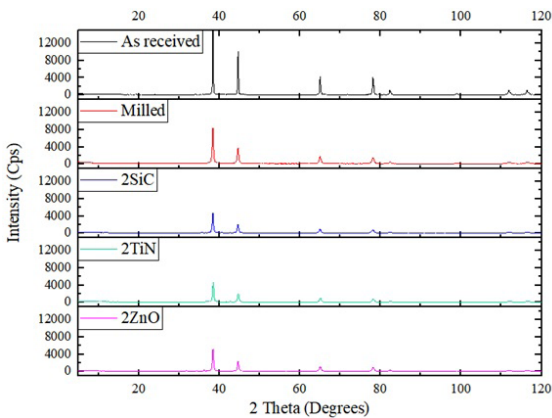


Figure 4. Diffractograms of AA7075 As received, Milled, Milled with 2 wt% SiC, TiN, and ZnO nano-reinforcements.

The process observes similar values among AA7075 milled, AA7075 plus 2wt% of TiN or ZnO. The crystallite and particle size values for the sample AA7075 plus 2 wt% of SiC were superior because of less micro deformation found.

The SEM (Figures 6-9) shows an almost spherical morphology for the as-received powders from the gas-atomized

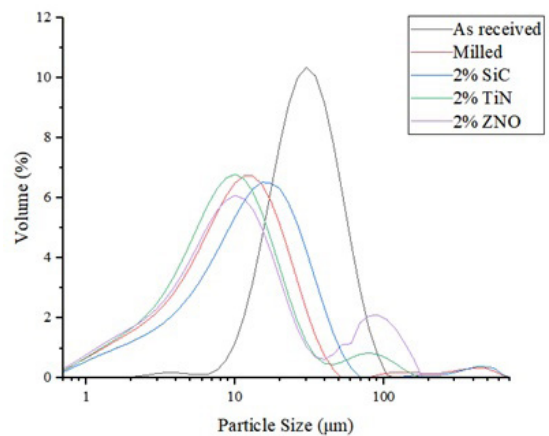


Figure 5. Particle size distribution of AA7075: As received, Milled, Milled with 2 wt% SiC, TiN, and ZnO nano-reinforcements.

manufacturing process. After milling, small rounded and flat particles show a quasi-equilibrium state found for all cases.

The milling efficiency depends on the characteristics like mechanical parameters applied, the medium used, type, and percentage of reinforcements and alloy elements³⁷. Wet milling provides relatively small stress and temperature, and distributes the reinforcement to the whole system, while the energetic conditions (high milling time, rotation speed, and BPR) produce the balanced morphology of the particle^{38,39}.

The microanalysis of EDS (Table 3 and Figures 10-14) indicates that alcohol liquid promotes the rise of oxygen percentual. No contamination from the steel balls and the stainless steel attritor mill was detected.

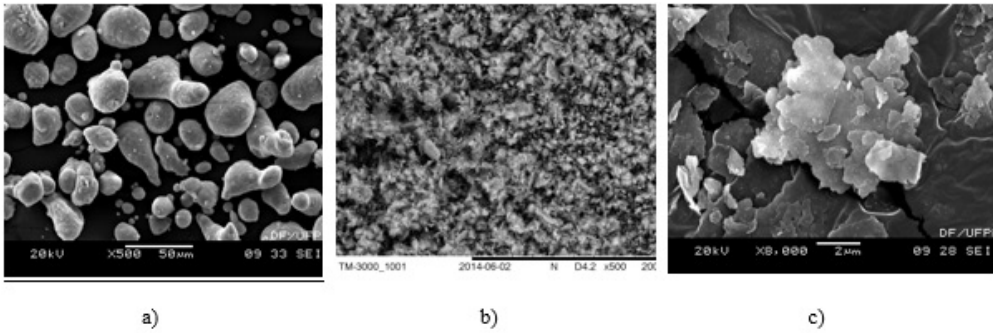


Figure 6. SEM AA7075 As received at 500x (a); A7075 Milled at 500x(b) and 8000x(c).

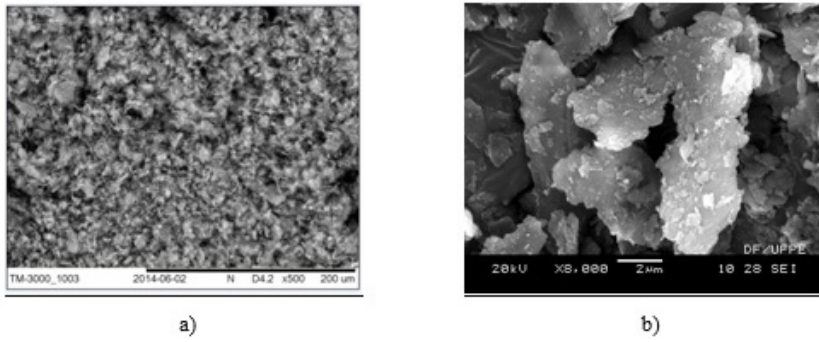


Figure 7. SEM AA7075 Milled + 2 % SiC at 500x (a) and 8000x (b).

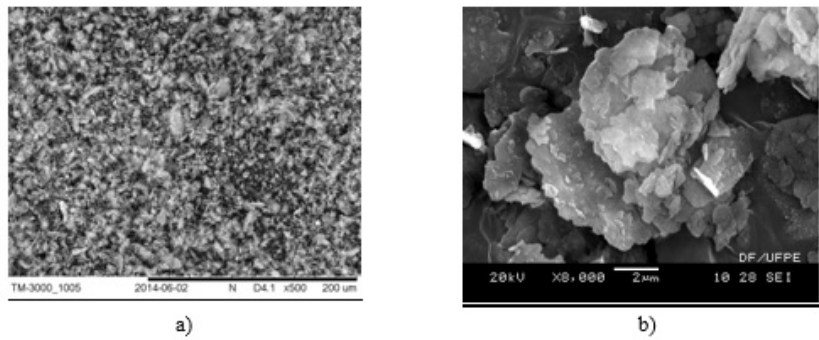


Figure 8. SEM AA7075 Milled + 2 % TiN at 500x (a) and 8000x (b).

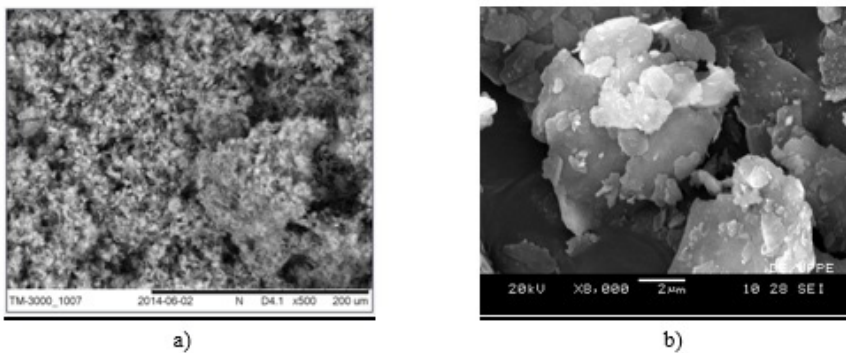


Figure 9. SEM AA7075 Milled + 2 % ZnO at 500x (a) and 8000x (b).

Table 3. Microanalyses of EDS AA7075.

Element	As received		Milled		Milled + 2 % SiC		Milled + 2 % TiN		Milled + 2 % ZnO	
	Weight (%)	Error	Weight (%)	Error	Weight (%)	Error	Weight (%)	Error	Weight (%)	Error
Aluminum	89.90	±3.9	69.90	±3.9	73.79	±2.8	65.85	±2.7	69.88	±2.8
Oxygen	3.84	±0.8	23.84	±0.8	20.57	±2.8	26.13	±4.3	23.53	±3.7
Magnesium	2.30	±0.1	2.10	±0.1	2.04	±0.1	1.82	±0.1	2.07	±0.1
Zinc	3.96	±0.1	3.87	±0.1	2.51	±0.1	3.42	±0.1	4.52	±0.2
Silicon	-	-	-	-	1.09	±0.1	-	-	-	-
Titanium	-	-	-	-	-	-	0.74	±0.0	-	-
Nitrogen	-	-	-	-	-	-	2.04	±1.1	-	-

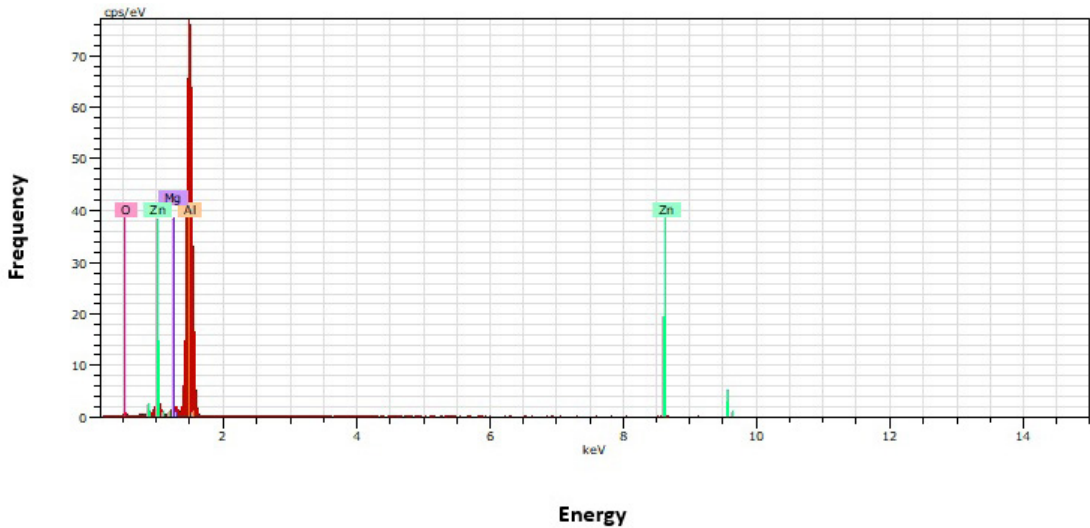


Figure 10. EDS AA7075 As received.

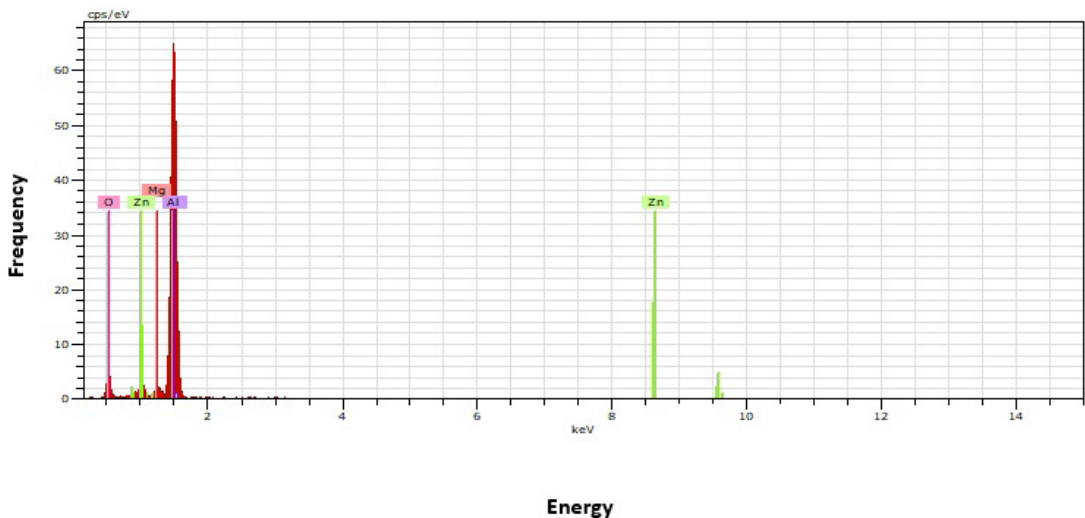


Figure 11. EDS AA7075 Milled.

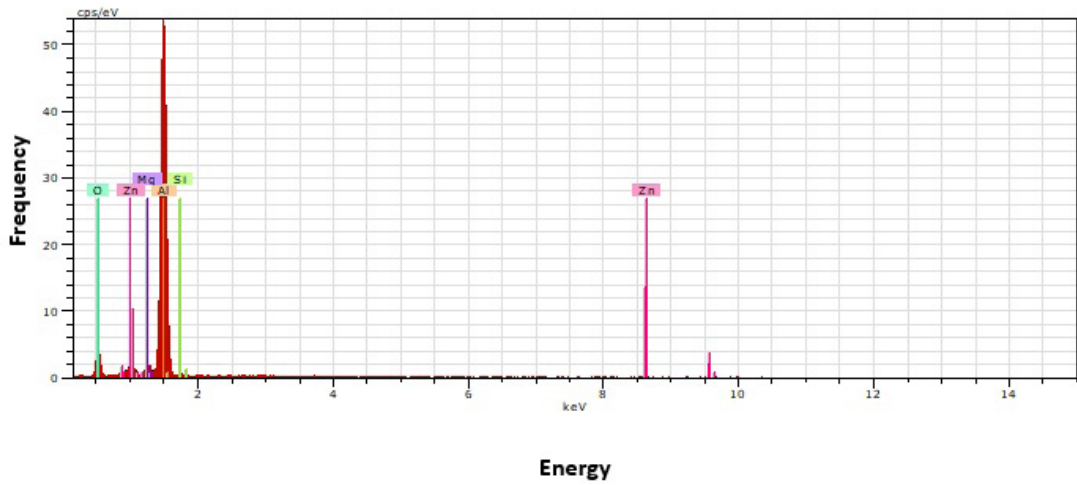


Figure 12. EDS AA7075 Milled + 2 % SiC.

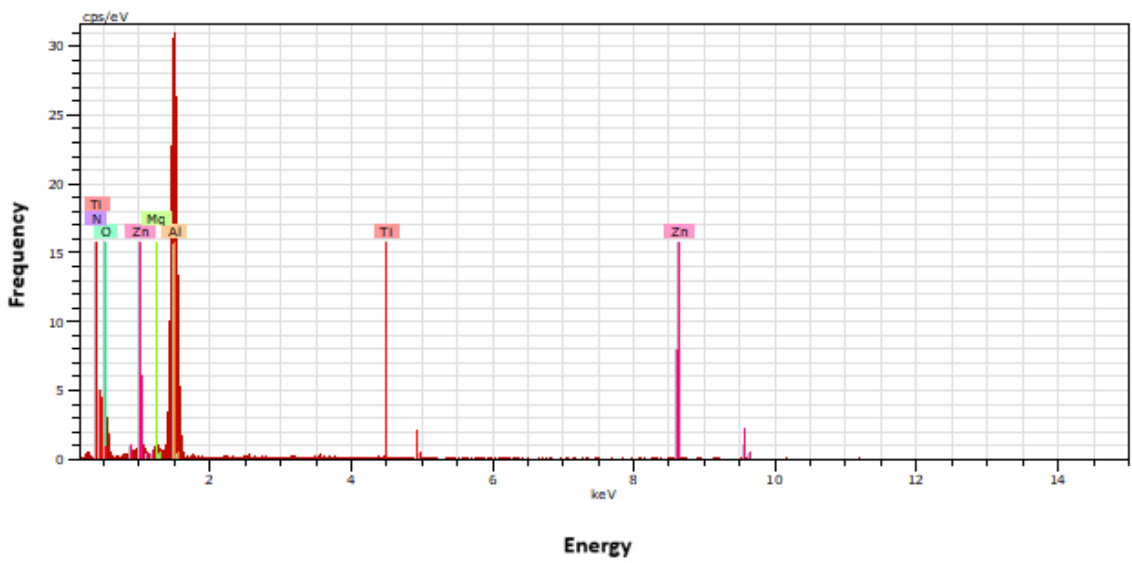


Figure 13. EDS AA7075 Milled + 2 % TiN.

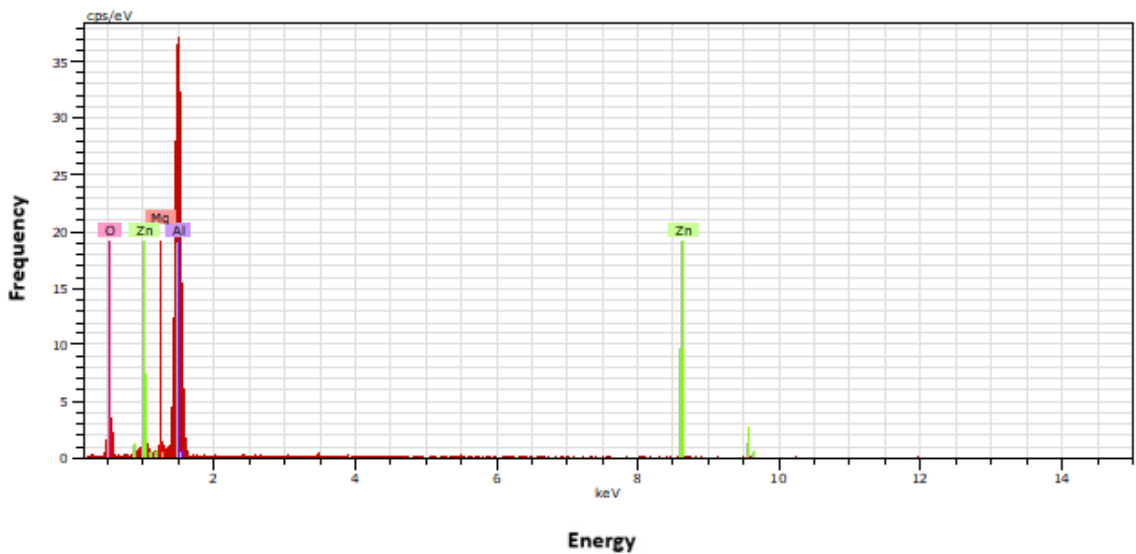


Figure 14. EDS AA7075 Milled + 2 % ZnO.

3.2. Characterization of extruded bars

Figure 15 shows the diagram of the relationship between the applied force and the displacement of the piston during the extrusion of all materials. For the composites and powder AA7075 milled, the forces required to extrude the bars (800 kN) were more significant than the ones found to extrude the powder AA7075 as received (540 kN). However, the crystallite decreased after milled, so the microhardness increased due to the Hall-Petch effect. The reinforcements also give extra resistance to the AA7075 milled powders changing the forces to extrude. The TiN reinforcement is the one that promotes higher force due probably to an increase of the friction between particles by its chemical nature and initial size of 20 nm.

Figure 16 shows a significant difference among the diffractograms of the specimens extruded compared to diffractograms of powders samples AA7075 (Figure 4). The bars extruded maintain the same peaks found at the origin powders, except for an increase of intensity from the crystallite size growth and an amorphous phase indicator at 20° degrees. The amorphous phase reduces the intensity of the diffraction peak when compared to the crystalline response due to the characteristics applied to the extrusion process (extrusion rate of 25:1, temperature of 450 °C / 2 minutes, extrusion speed of 1 mm/s). These parameters provide great frictional forces during extrusion and promote less homogeneous structural changes⁴⁰. Specifically, the Al secondary reflections of AA7075 as received, reduced due to significant changes in the structure of the spectrum, suggesting that the portion of alloying elements was dissolved in the matrix to form a solid solution. Therefore, there is a critical temperature at which grain growth decrease due to pre-existing alloy precipitates acting as a barrier in the matrix. With the increase in temperature by extrusion, there is the dissolution of precipitates considered anchors of the grain boundaries^{41,42}.

According to Table 4, crystallite size grows about ninety percent of the value found in powders except for the as-received one. The results indicate that the composite extruded bars and the AA7075 milled extruded bar have less thermal stability than the bar of AA7075 as-received because the crystallite size is inversely proportional to the volumetric modulus and an increase in temperature⁴³.

The SEM micrographs (Figure 17) show a fine microstructure and good consolidation for all milled extruded bars, except for AA7075 as-received. In this case, the bar was deformed heterogeneously, and superficial agglomerates formed in the extrusion direction due to the thermal stability found.

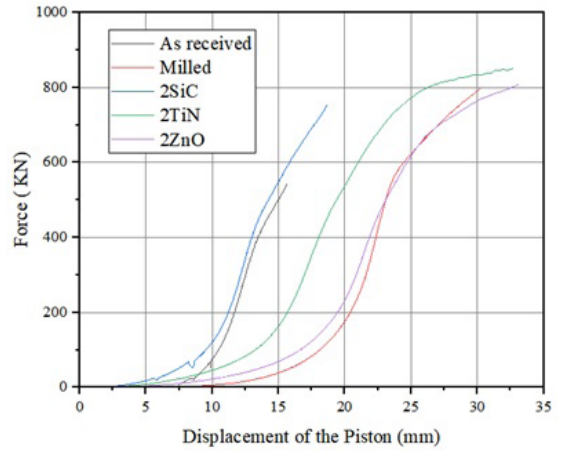


Figure 15. Force VS Piston displacement for all powders.

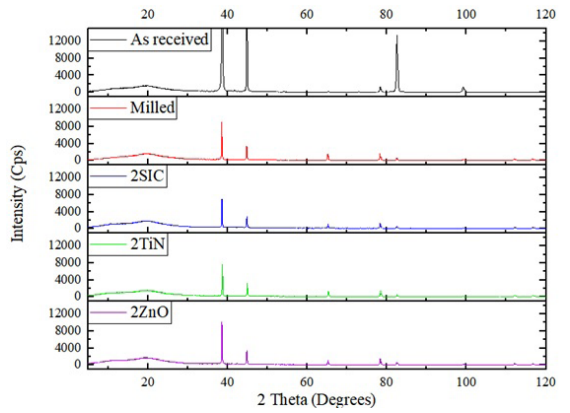


Figure 16. Diffractograms of AA7075-based extruded bars.

Table 5 shows that high-energy ball milling increases powders' microhardness from 21 % to 52 % compared to the as-received material. The results suggest the combination of two mechanisms related to the microhardness of extruded composites: the reduction of crystallite size and the inhibition of the movement of dislocations by the dispersion of reinforcements originating from the milling process^{44,45}. The highest hardness values are related to the smaller crystallite sizes obtained after extrusion and the kind of reinforcement used.

Table 4. Values of crystallite size for all billets extruded.

Samples	Powder Crystallite Size [nm]	Billet Extruded Crystallite Size [nm]	Relative Percentage [%]	Reinforce
AA7075 As received	49	67	36.73	No
AA7075 Milled	29	54	86.20	No
AA7075 Milled + 2 % SiC	32	62	93.75	2 % SiC
AA7075 Milled + 2 % TiN	29	53	82.75	2 % TiN
AA7075 Milled + 2 % ZnO	30	59	96.67	2 % ZnO

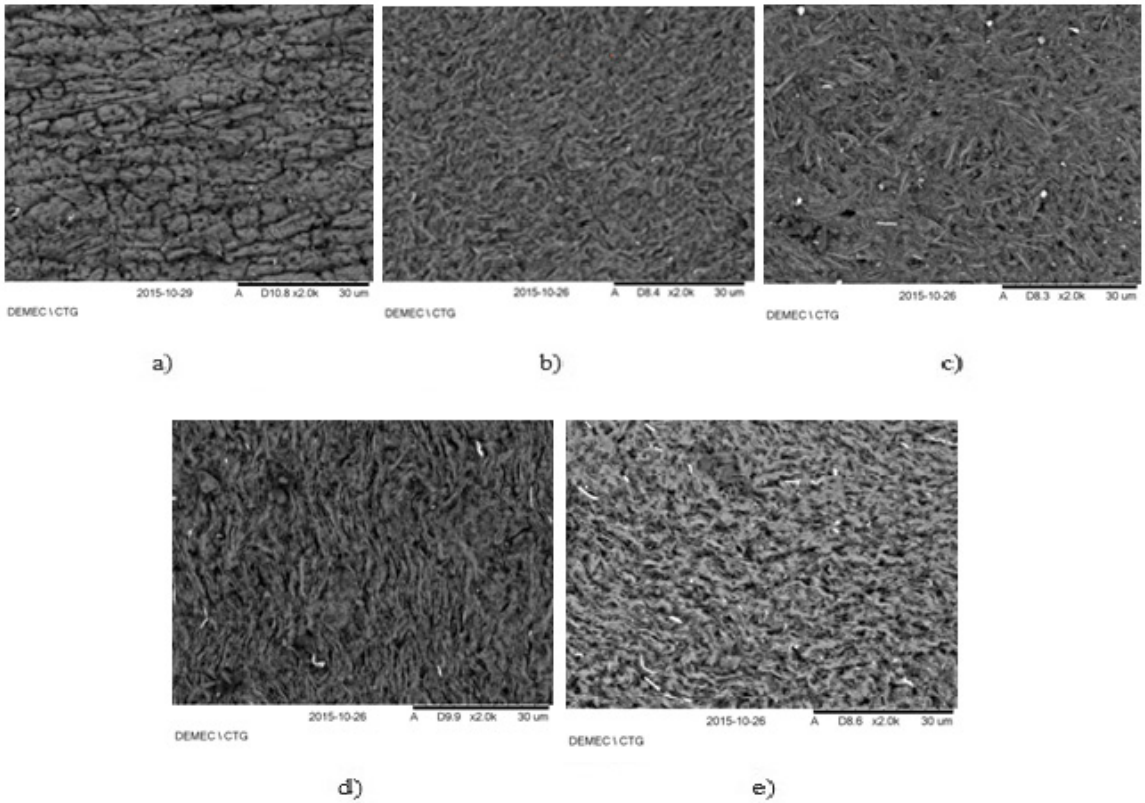


Figure 17. SEM billets extruded AA7075 (2000x): As received (a); Milled (b); Milled + 2 % SiC (c); Milled + 2 % TiN (d); Milled + 2 % ZnO (e).

Table 5. Values of microhardness Vickers for all extruded bars.

Samples	Microhardness Vickers	
	HV 0.05	Increment Percentage
AA7075 As received	$(80 \pm 2.97)_{95\%p}$	-
AA7075 Milled	$(120.75 \pm 4.03)_{95\%p}$	50.93 %
AA7075 Milled + 2 % SiC	$(97.27 \pm 2.75)_{95\%p}$	21.58 %
AA7075 Milled + 2 % TiN	$(121.60 \pm 4.69)_{95\%p}$	52.00 %
AA7075 Milled + 2 % ZnO	$(113.17 \pm 7.33)_{95\%p}$	41.46 %

4. Conclusions

Powders of AA7075 unreinforced and reinforced by nanosized particles of SiC, ZnO, and TiN in 2 wt% were produced by high-energy ball milling, and bars were extruded with relative success. The results can be resumed as follows:

1. For all samples of milled powders, the crystallite and particle sizes achieved values of the same magnitude independent of reinforcement, about 30 nm and 10 µm, respectively.
2. Small rounded and flat particle powders show a quasi-equilibrium state achieved, and no contamination from the steel balls and the stainless steel attritor mill was detected.
3. All extruded bars obtained a fine microstructure and good consolidation, except for AA7075 as-received, which was deformed heterogeneously,

and superficial agglomerates were formed in the extrusion direction.

4. The highest hardness values are related to the smaller crystallite sizes obtained after extrusion and the kind of reinforcement used.

5. Acknowledgments

This work has been carried out under the projects: “Functional” - Partnership between the Federal University of Pernambuco and European Union’s Seventh Framework Programme for Research and “Aluminum Metal Matrix Composite Ceramic Particulate Reinforcement” of the Federal Rural University of Pernambuco, National Council for Scientific and Technological Develop (CNPq) - Brazil and Pernambuco Science and Technology Support Foundation (FACEPE) - Brazil.

6. References

- Garg P, Jamwal A, Kumar D, Sadasivuni KK, Hussain CM, Gupta P. Advance research progress in aluminum matrix composite: manufacturing & applications. *J Mater Res Technol.* 2019;8(5):4924-39. <http://dx.doi.org/10.1016/j.jmrt.2019.06.028>.
- Barbedo EL, Gonçalves PH, Lamoglia MS, Pontes AMP, Kuffner BHB, Gomes GF, et al. Analysis of milling efficiency of the vanadis 8 tool steel with additions of vanadium and molybdenum carbides. *Mater Res.* 2021;24(5):e20210054. <http://dx.doi.org/10.1590/1980-5373-MR-2021-0054>.
- Gu Y, Yi M, Cheng Y, Tu J, Zhou Z, Luo J. Effect of the mount of SiC particle on the microstructure, mechanical and wear properties of FeMnCoCr high entropy alloy composites. *Mater Charact.* 2022;193:112300. <http://dx.doi.org/10.1016/j.matchar.2022.112300>.
- Hernandezbattez A, Gonzalez R, Viesca J, Fernandez J, Diazfernandez J, Machado A, et al. CuOZrO₂ and ZnO nanoparticles as antiwear additive in oil lubricants. *Wear.* 2008;265(3-4):422. <http://dx.doi.org/10.1016/j.wear.2007.11.013>.
- Zhong Y, Shaw LL, Manjares M, Zawrah MF. Synthesis of silicon carbide nanopowder using silica fume. *J Am Ceram Soc.* 2010;93(10):3159. <http://dx.doi.org/10.1111/j.1551-2916.2010.03867.x>.
- Gong X, Wang B, He Y, Zhu Q. TiN-SiO₂ double layer composite coating with enhanced oxidation resistance and reusability in anti-coking applications. *Fuel.* 2022;324(C):124808. <http://dx.doi.org/10.1016/j.fuel.2022.124808>.
- Akinribide OJ, Ogundare OB, Akinwamide SO, Gamaoun F, Olubambi PA. Alloying effect of copper in AA-7075 aluminum composite using bale out furnace. *J Mater Res Technol.* 2022;18:3849-56. <http://dx.doi.org/10.1016/j.jmrt.2022.04.054>.
- Bamberg P, Gintrowski G, Liang Z, Schebian A, Reisgen U, Precoma N, et al. Development of a new approach to resistance spot weld AA-7075 aluminum alloys for structural applications: an experimental study e Part 1. *J Mater Res Technol.* 2021;15:5569-81. <http://dx.doi.org/10.1016/j.jmrt.2021.10.142>.
- Chen C, Sun C, Wang W, Qi M, Han W, Li Y, et al. Microstructure and mechanical properties of in-situ TiB₂/AlSi₇Mg composite via powder metallurgy and hot extrusion. *J Mater Res Technol.* 2022;19:1282-92. <http://dx.doi.org/10.1016/j.jmrt.2022.05.117>.
- Rahimian M, Ehsani N, Parvin N, Reza Baharvandi H. The effect of particle size, sintering temperature and sintering time on the properties of Al-Al₂O₃ composites, made by powder metallurgy. *J Mater Process Technol.* 2009;209(14):5387-93. <http://dx.doi.org/10.1016/j.jmatprotec.2009.04.007>.
- Chen C, Li F, Han W, Lu T, Li P, Cui Q, et al. Thermally stable Al conductor prepared from Al powder with a low oxygen content. *Mater Sci Eng A.* 2021;813:141174. <http://dx.doi.org/10.1016/j.msea.2021.141174>.
- Rane AV, Kanny K, Abitha VK, Thomas S. Chapter Title. In: Surname N, editor. *Synthesis of inorganic nanomaterials: methods for synthesis of nanoparticles and fabrications of nanocomposites.* Sawston: Woodhead Publishing; 2018. p. 121-139
- Fecht HJ. Nanostructure formation by mechanical attrition. *Nanostruct Mater.* 1995;6:33-42. [http://dx.doi.org/10.1016/0965-9773\(95\)00027-5](http://dx.doi.org/10.1016/0965-9773(95)00027-5).
- Mendonça CSP, Oliveira AF, Oliveira LA, Siva MR, Melo MLNM, Silva G. Structural and magnetic properties of duplex stainless steel (UNS S31803) powders obtained by high energy milling of chips with additions of NBC. *Mater Res.* 2018;21(1):e20170717. <http://dx.doi.org/10.1590/1980-5373-MR-2017-0717>.
- Sayed A, Sherbini A, Bakr M, Ghoneim I, Saad M. Exfoliation of graphene sheets milling of graphite in 2-ethylhexanol and kerosene. *J Adv Res.* 2017;8(3):209-15. <http://dx.doi.org/10.1016/j.jare.2017.01.004>.
- Suryanarayana C. Mechanical alloying and milling. *Prog Mater Sci.* 2001;46:1-184. [http://dx.doi.org/10.1016/S0079-6425\(99\)00010-9](http://dx.doi.org/10.1016/S0079-6425(99)00010-9).
- Shtansky DV, Matveev AT, Permyakova ES, Leybo DV, Konopatsky AS, Sorokin PB. Recent progress in fabrication and application of BN nanostructures and BN-based nanohybrid. *Nanomaterial.* 2022;12:2810. <http://dx.doi.org/10.3390/nano12162810>.
- Chen C, Wang W, Guo Z, Sun C, Volinsky AA, Paley V. Annealing effects on microstructure and mechanical properties of ultrafine-grained Al composite reinforced with nano-Al₂O₃ by rotary swaging. *J Mater Eng Perform.* 2018;27(4):1738-45. <http://dx.doi.org/10.1007/s11665-018-3301-2>.
- Balog M, Simancik F, Walcher M, Rajner W, Poletti C. Extruded Al-Al₂O₃ composites formed in situ during consolidation of ultrafine Al powders: effect of the powder surface area. *Mater Sci Eng A.* 2011;529:131-7. <http://dx.doi.org/10.1016/j.msea.2011.09.006>.
- Barador A, Issatiyapat A, Umeda J, Yamanoglu R, Prunco C, Amrin A, et al. Strength-ductility balance of powder metallurgy Ti-2Fe-2W alloy extruded at high-temperature. *J Mater Res Technol.* 2021;14:677-91. <http://dx.doi.org/10.1016/j.jmrt.2021.06.086>.
- Araujo OO Fo, Araújo ER, Lira HM, Gonzales CH, Silva NDG, Urtiga SP Fo. Manufacturing of AA2124 aluminum alloy metal matrix composites reinforced by silicon carbide processed by powder metallurgy techniques of high energy ball milling and hot extrusion. *Mater Sci Forum.* 2017;899:25-30. <http://dx.doi.org/10.4028/www.scientific.net/MSF.899.25>.
- Ikumapayi OM, Oyinbo ST, Bodunde OP, Afolalu SA, Okokpujie IP, Akinlabi ET. The effects of lubricants on temperature distribution of 6063 aluminum alloy during backward cup extrusion process. *J Mater Res Technol.* 2019;8(1):1175-87. <http://dx.doi.org/10.1016/j.jmrt.2018.08.006>.
- Lira HM, Rodrigues PR, Araujo OO Fo, Gonzales CH, Urtiga SP Fo. Nanostructured al powder obtained by high energy ball milling at ambient and cryogenic temperatures. *Mater Sci Forum.* 2014;802:125-9. <http://dx.doi.org/10.4028/www.scientific.net/MSF.802.125>.
- Cruz S, Rey P, Román M, Merino P. Influence of content and particle size on properties of TiC reinforced 7075 aluminum matrix composite. In *15th European Conference on Composite Materials*; 2012; Venice, Italy. Proceedings. Italy: University of Padova; 2012. p. 1-8.
- Pohanish R. *Sittig's handbook of toxic and hazardous chemicals and carcinogens.* 7th ed. Oxford: Elsevier; 2017. 1-0460; p. 1820-906. <https://doi.org/10.1016/B978-0-323-38968-6.00009-0>.
- Thomas S, Kalarikkal N, Abraham AR. Design, fabrication and characterization of multifunctional nanomaterials. Amsterdam: Elsevier; 2021. <https://doi.org/10.1016/C2019-0-00948-X>
- Monshi A, Foroughi MR, Monshi MR. Modified scherrer equation to estimate more accurately nano-crystallite size using XRD. *World Journal of Nano Science and Engineering.* 2012;2:154-60.
- Svensson DN, Messing I, Barron J. An investigation in laser diffraction soil particle size distribution analysis to obtain compatible results with sieve and pipette method. *Soil Tillage Res.* 2022;223:105450. <http://dx.doi.org/10.1016/j.still.2022.105450>.
- ISO: International Organization for Standardization. ISO 13320: Particle Size Analysis-Laser Diffraction Methods. London: ISO; 2020.
- Jesus LCC, Brandão SM, Grossi LJ, Mutterle PV, Luz SM, Saraiva I. Influência dos parâmetros de pressão e compactação e tempo de moagem na obtenção da liga Al4Cu pelo processo da metalurgia do pó. *Revista Interdisciplinas de Pesquisa em Engenharia.* 2019;5(2):100-12. <http://dx.doi.org/10.26512/ripe.v5i2.26872>.
- Ferguson BL, Roberts PR. Extrusion of metal powders. In: Lee PW, Trudel Y, Iacocca R, German RM, Ferguson BL, Eisen WB, et al., editors. *Powder metallurgy technologies and applications.* United States: ASM International; 1998. Vol. 7; p. 1461-88.

32. Hattori CS, Almeida GFC, Gonçalves RLP, Santos RG, Souza RC, da Silva WC, et al. Microstructure and fatigue properties of extruded aluminum alloys 7046 and 7108 for automotive applications. *Journal of Materials and Technology*. 2021;14:2970-81. <http://dx.doi.org/10.1016/j.jmrt.2021.08.085>.
33. Ngembamrung S, Suzuki Y, Takatsuji N, Dohda K. Investigation of surface cracking of hot-extruded AA7075 billet. *Procedia Manuf*. 2018;15:217-24. <http://dx.doi.org/10.1016/j.promfg.2018.07.212>.
34. Zhu HL, Han QX, Wu J, Meng XL, Cui HZ. Large scale synthesis of nanoporous BN flake with high surface area. *J Cryst Growth*. 2016;434:19-24. <http://dx.doi.org/10.1016/j.jcrysgro.2015.10.021>.
35. ASTM: American Society for Testing and Materials. ASTM E-384: Standard test method for knoop and vickers hardness of materials. United States: ASTM International; 2017.
36. Cao W. High energy ball milling process for nanomaterial synthesis [Internet]. Skyspring Nanomaterials, 2022 [cited 2023 Feb 28]. Available from: <https://www.understandingnano.com/nanomaterial-synthesis-ball-milling.html>
37. Kamrani S, Riedel R, Reihani SMS, Kleebe HJ. Effect of reinforcement volume fraction on the mechanical properties of Al SiC nanocomposites produced by mechanical alloying and consolidation. *J Compos Mater*. 2010;313:44. <http://dx.doi.org/10.1177/002199830934757>.
38. Jung HJ, Sohn Y, Sung HG, Hyund HS, Shin WG. Physicochemical properties of ball milled boron particles: dry vs. wet ball milling process. *Powder Technol*. 2015;269:548-53. <http://dx.doi.org/10.1016/j.powtec.2014.03.058>.
39. Ji YY, Xu YZ, Zhang BB, Behnamian Y, Xia DH, Hu WB. Review of micro-scale and atomic-scale corrosion mechanisms of second phases in aluminum alloys. *Trans Nonferrous Met Soc China*. 2021;31(11):3205-27.
40. Srisuriyacho J, McNair SAM, Chen Y, Barthelay T, Gray R, Benézéch J, et al. Carbon fiber lattice strain mapping via microfocous synchrotron x-ray diffraction of a reinforce composite. *Carbon*. 2022;200:347-60. <http://dx.doi.org/10.1016/j.carbon.2022.08.041>.
41. Peres MM, Fogagnolo JB, Bolfarini C, Kiminani CS, Botta WJ Fo, Jorge AM Jr. Hot extrusion of nanostructured aluminum powder alloys: precipitation effect on the microstructure control. *Tecnol Metal Mater Min*. 2010;7(1-2):6-11. <http://dx.doi.org/10.4322/tmm.00701002>.
42. Stopyra W, Gurber K, Smolina I, Kurzynowski T, Kuznicka B. Laser powder bed fusion of AA7075 alloy: influence of process parameters on porosity and hot cracking. *Addit Manuf*. 2020;35:101270. <http://dx.doi.org/10.1016/j.addma.2020.101270>.
43. Mohamed FA, Xun Y. Correlations between the minimum grain size produced by illing and material parameters. *Mater Sci Eng*. 2003;345A:133-9. [http://dx.doi.org/10.1016/S0921-5093\(02\)00936-X](http://dx.doi.org/10.1016/S0921-5093(02)00936-X).
44. Marim MM, Camacho AM, Pérez JA. Influence of temperature on AA6061 aluminium alloy in a hot extrusion process. *Procedia Manuf*. 2017;13:327-443. <http://dx.doi.org/10.1016/j.promfg.2017.09.084>.
45. Lara RD, Guel IE, Ruiz GH, Campos RF, Ramirez JMH, Sánchez RM. Synthesis of aluminum alloy 7075-grafite composites by milling process and hot extrusion. *J Alloys Compd*. 2011;509s:284-9. <http://dx.doi.org/10.1016/j.jallcom.2010.11.183>.